Trends in Satellite-Observed Circumpolar Photosynthetic Activity from 1982 to 2003: The Influence of Seasonality, Cover Type, and Vegetation Density

Andrew G. Bunn* and Scott J. Goetz

Woods Hole Research Center, Falmouth, Massachusetts

Received 2 January 2006; accepted 2 March 2006

ABSTRACT: Time series analyses of a 22-yr record of satellite observations across the northern circumpolar high latitudes were conducted, and trends in vegetation photosynthetic activity were assessed using a series of statistical tests. The results indicate that most of the northern circumpolar high latitudes (>85%) showed no significant trend in vegetation activity despite systematic climate warming during the period of analysis. Of the areas that did change, many showed the expected trends in "greening" of vegetation activity. There were, however, significant differences in the magnitude and even in the direction of trends when stratified by vegetation type and density. Tundra areas consistently and predominantly showed greening trends. Forested areas showed declines in activity ("browning") in many areas, and these were systematically higher in areas with denser tree cover—whether deciduous or evergreen, needle- or broad-leafed. The seasonality of the trends was also distinct between vegetation types, with a divergence in trends between late spring and early summer (positive) versus late summer (negative) portions of the growing sea-

* Corresponding author address: Dr. Andrew G. Bunn, Woods Hole Research Center, 149 Woods Hole Rd., Falmouth, MA 02540-1644.

E-mail address: abunn@whrc.org

sons in forested areas. In contrast, tundra and other predominantly herbaceous areas showed positive trends in all portions of the growing season. These results confirm recent findings across the high latitudes of North America and are supported by an increasing array of in situ measurements. They indicate that the boreal forest biome might be responding to climate change in previously unexpected ways, and point to a need for an expanded observational network, additional analysis of existing datasets (e.g., tree rings), and improvements in process models of ecosystem responses to climate change.

KEYWORDS: Global change; Boreal; Remote sensing

1. Introduction

Since 1981, the time series observations of vegetation activity from the Advanced Very High Resolution Radiometers (AVHRR) on board National Oceanic and Atmospheric Administration (NOAA) spacecraft have been critical for global change research. In particular, the composite normalized differenced vegetation index (NDVI) data have been widely used to document widespread increases in photosynthesis ("greening") in many parts of the world (Myneni et al. 1997; Zhou et al. 2001; Slayback et al. 2003). Such changes have been associated with modification of the global carbon cycle (Keeling et al. 1996; Nemani et al. 2003). Two recent studies, however, have described declines in photosynthetic activity across the northern extratropics generally, and above 50°N especially, despite increasing temperatures (Angert et al. 2005; Goetz et al. 2005). Over the period 1981–2003 large areas of boreal forest experienced little change, but many others displayed decreasing photosynthetic activity ("browning"). Tundra areas, in contrast, almost exclusively underwent greening, as had been suggested by the earlier studies. Model analysis indicates that the boreal forest browning might be due to temperature-related water stress in the later part of the summer, which offset photosynthetic gains made in the early part of the summer (Angert et al. 2005). This is supported by analyses of seasonal climate variables and photosynthetic activity in Canada that show evergreen coniferous forest responding positively to higher spring minimum temperatures while tundra areas respond to summer maximum temperatures (Bunn et al. 2005).

In the high latitudes, warming is generally thought to increase plant activity and subsequently increase terrestrial carbon storage (Cox et al. 2000; Dufresne et al. 2002). Indeed, documenting and characterizing high-latitude carbon storage patterns in response to climate variability are seen as crucial to understanding the global carbon budget (Gorham 1991; Bonan et al. 1992; Myneni et al. 1995). The recent documentation of photosynthetic activity at high latitudes has not, however, made full use of the spatial extent (Goetz et al. 2005) or resolution (Angert et al. 2005) of the AVHRR–NDVI record. Nor has recent analysis adequately made use of ancillary data derived from remote sensing that might help interpret patterns in the trends by land-cover type or vegetation density.

Cover type and the proportion of plant functional types (e.g., herbaceous and woody) provide a quantitative, biophysical framework to interpret photosynthetic trends. Our objective in this paper was to characterize circumpolar trends (above 50°N) in vegetation activity by vegetation type and density over the entire growing

season (May–August) as well as the early (May and June) and late portions (July and August) of the growing season separately.

2. Study area and data

We considered all land surfaces above 50°N in this study except the glaciated areas of Greenland. This encompasses approximately 3400×10^6 ha, about three-quarters of which is located in Russia and Canada (1800 and 1000×10^6 ha, respectively). We used three primary datasets derived from polar-orbiting satellites: 1) a time series of AVHRR–NDVI from 1982–2003, 2) vegetation density from the vegetation continuous fields product derived from the Moderate Resolution Imaging Spectroradiometer (MODIS) sensor, and 3) the global land-cover classification for the year 2000 (GLC2000) derived from the *SPOT4* VEGETATION sensor. Links to the datasets used are provided in Table 1.

The AVHRR–NDVI data were produced as part of the NASA Global Inventory, Monitoring and Modeling project (GIMMS version-G). This recent product has been calibrated to account for orbital drift, cloud cover, sensor degradation, and the emission of volcanic aerosols (Brown et al. 2004; Tucker et al. 2006). Spectral vegetation indices like the NDVI have been used to estimate a wide range of Earth surface variables since early field work in controlled experiments (Richardson and Wiegand 1977; Tucker 1979), particularly the fraction of photosynthetically active radiation absorbed by green vegetation (Fpar) and leaf area index (LAI; Asrar et al. 1984; Spanner et al. 1990; Goel and Qin 1994). Temporally integrated NDVI has been shown to be closely related to annual biomass production in herbaceous vegetation (Tucker et al. 1981; Asrar et al. 1985; Daughtry et al. 1992), and it has been suggested that this extends across vegetation types (Field 1991) despite differences in respiratory costs (Ryan et al. 1997; Goetz and Prince 1998). At these coarse spatial scales (64 km^2 cells) and short temporal scales (15-day composite images), NDVI appears to be most closely related to gross photosynthesis (Pg) rather than net production (Sellers 1987; Myneni et al. 1995; Goetz and Prince 1999; Turner et al. 2003). Thus, we scaled the NDVI data between the 5% and 95% percentile values and used a linear transform of NDVI to relative Pg ranging from zero to one (0–1) (Goetz et al. 2005). These data, and all spatial data in this study, were transformed to a stereographic polar projection based on the Clarke 1866 spheroid, with units in meters.

Table 1. Primary datasets used.

Dataset	Nominal spatial resolution	Original projection*	Available online
GIMMS–NDVI Version-G	8 km × 8 km	Albers Conical Equal Area	http://glcf.umiacs.umd.edu/data/gimms/
MODIS VCF*	500 m × 500 m	Goode's Homolosine	http://glcf.umiacs.umd.edu/data/modis/vcf/
GLC2000 Land Cover Map**	~1 km × 1 km	Geographic	http://www-gvm.jrc.it/glc2000/

* All datasets were reprojected to a stereographic polar projection by resampling via cubic convolution for the GIMMS and MODIS VCF datasets and nearest-neighbor assignment for the GLC2000 dataset.

** Resampled to 8 km × 8 km as described in the text.

Proportional estimates of Earth surface cover for two broad categories of plant functional types (i.e., trees and herbaceous plants) as well as nonvegetated cover (i.e., bare ground) were obtained using the MODIS Vegetation Continuous Fields (VCF) datasets. These data have global coverage at 500-m resolution and have been validated in a range of environments (M. C. Hansen et al. 2005; but also see Defries et al. 2000; M. C. Hansen et al. 2002a,b). Each 500-m pixel contains the proportion of woody vegetation, herbaceous vegetation, and bare ground cover as estimated using 32-day composites of MODIS observation from 2000 and 2001. These three cover types sum to one (100%) for each grid cell location. Both the MODIS–VCF and the GIMMS–NDVI data are available from the Global Land Cover Facility (Table 1).

Land-cover data were obtained from the GLC2000 from the Joint Research Center (Bartalev et al. 2003; Latifovic et al. 2004). The classification was produced using 14 months of daily imagery from the VEGETATION instrument on board the *SPOT4* satellite. The period covered by the daily imagery was from November 1999 through December 2000 and the spatial resolution was 1 km. Land-cover classifications were performed for different sections of the globe separately and combined into a single cohesive image. We compared the GLC2000 map to other land-cover maps, including the MODIS land-cover product [International Geosphere–Biosphere Program (IGBP) schema available at http://glcf.umiacs.umd.edu], and found them to be well correlated at the class level. This was consistent with the recent findings of Giri et al. (Giri et al. 2005). For our purposes, however, the products were qualitatively similar for North America but differed substantially in Russia, particularly in terms of the extent of needle-leaved deciduous tree cover. The differences result largely from the percent of tree cover necessary for a "forest" classification. The GLC2000 classification scheme allows an area to be classified as forest with as little as 10% of the pixel occupied by trees. These wide expanses of low-density needle-leaved deciduous forest over eastern Russia are consistent with other forest cover maps that show vast expanses of "sparse larch" that correspond well with the GLC2000 map (Nikolauk 1973; Aksenov et al. 2002). Although classifying areas with very low density of trees as forest contains obvious pitfalls for some applications, for example, carbon process modeling, the incorporation of the tree density data from the MODIS VCF allowed us to determine the proportion of forest in a given cell and stratify the AVHRR time series analysis, described below, by both vegetation cover type and density.

3. Data processing and statistical modeling

A time series (y_t) of mean growing-season Pg was calculated for each cell from 1982 to 2003 (1981 was not used because no data exist prior to July 1981). We defined the growing season as May to August in this study but also analyzed early and late growing season periods. The definition of the growing season is somewhat subjective over such a large extent and varied terrain. For the analysis reported here, we selected a May to August window for two reasons: 1) the GIMMS dataset contains many no-data values at high latitudes for all periods prior to May and after August, making unbiased average growing season problematic to calculate; and 2) instrumental field measurements of canopy light harvesting (i.e., Fpar) in

interior Alaska (63°50′N, 145°30′W) from 2002 to 2005 indicate the onset of boreal forest green-up in early May followed by rapid senescence after August (Steinberg et al. 2006). We further divided the growing season into early (May–June) and late (July–August) periods and then analyzed all three characterizations of the growing season trends.

Each time series (y_t) was tested to determine if a significant deterministic trend existed over the time period (t) 1982–2003 ($y_t = \alpha + \beta t + \varepsilon_t$; $t = 1,2,3, \ldots, T$; H_0: $\beta = 0$; H_1: $\beta \neq 0$). If a significant trend ($p \leq 0.05$) was detected, then the slope (β) was extracted for the grid cell. We used three separate statistical tests to assess the significance of trends in Pg: Augmented Dickey Fuller (ADF) tests (Dickey and Fuller 1981), a nonparametric trend test (Siegel and Castellan 1988), and Vogelsang's $t\text{-}PS_T$ stationarity test (Vogelsang 1998; Fomby and Vogelsang 2002). All three of these tests have been used previously to assess trends in the AVHRR–NDVI data, and we refer readers to the aforementioned papers by Goetz et al. (Goetz et al. 2005) for information on the ADF tests and Vogelsang test, and Angert et al. (Angert et al. 2005) for an application of a nonparametric trend test. We found similar broad-scale patterns between all three trend tests (see the appendix) and elected to use Vogelsang's $t\text{-}PS_T$ stationarity test for the remainder of the study. The Vogelsang test is robust to spurious trends that might result from strong serial correlation in the time series and does not overreject the hypothesis of no trend when the serial correlation is strong, or if there is a unit root (or near unit root) in the errors (as some autoregressive modeling approaches do; Vogelsang 1998). Finally, the Vogelsang test does not require estimates of nuisance parameters stemming from uncertainty in the correlation structure of the data (Vogelsang 1998; Fomby and Vogelsang 2002).

The slopes (β) of significant time series (May–August, May and June, and July and August, separately) were modeled as a function of land cover and vegetation density using the GLC2000 map and the MODIS VCF described above. Both the predictor datasets required resampling, however, because of the finer spatial resolution as compared to the 64-km^2 resolution of the AVHRR data (Table 1). For the land-cover dataset, the most common cover type occurring in the 64-km^2 window was derived along with the number of different land-cover types present. The mean and standard deviations of the proportional vegetation types that occurred within each 64-km^2 grid cell were retained for use with the MODIS VCF datasets.

Slopes were modeled as a function of vegetation proportion and land cover. Specifically, all the significant slopes (β) were modeled as a function of the mean and standard deviation of the proportion of percent tree, percent bare, and percent herbaceous cover as well as the most common land-cover type and the variety of land-cover types present in each cell. We used a variety of exploratory data analyses (see section 5), and predictive models were built with ensembles of regression trees using Breiman and Cutler's random forests (RF) ensemble prediction method (Breiman 2001; Liaw and Wiener 2002). In the RF algorithm, many regression trees (typically hundreds) are constructed using different random samples of the data. Unlike most regression tree analysis, splits at each node are chosen from a randomly selected subset of all the available predictors at each node. The results are then aggregated, placing this technique in the family of bootstrap aggregation or "bagging" approaches to machine learning (Breiman 1996). Like other decision tree approaches, the RF algorithm can be used with mixed categori-

cal and continuous data—even highly correlated variables like the VCF components. Unlike some of the other ensemble approaches, for example, stochastic gradient boosting (Lawrence et al. 2004), the RF approach has two advantages. First, the RF algorithm requires only two parameters: the number of regression trees to grow and the number of variables to try at each split (Breiman 2001). The first parameter can be easily met with sufficient computing time and the second parameter is largely insensitive (Liaw and Wiener 2002). Second, model error is quantified with respect to the out-of-bag (OOB) error estimates. The OOB data are the portion of the data not drawn into the sample at each bootstrap iteration and provide an unbiased estimate of error. More specifically, the OOB data are the one-third of the input data that is randomly excluded from the construction of each of the trees, and that one-third is a different random selection for each tree. This allows the full dataset to be used and data need not be withheld for validation. (Liaw and Wiener 2002; Lawrence et al. 2006). The wide spatial distribution of the areas with significant trends largely precludes issues of spatial autocorrelation in performing the bootstrapping as the random samples are selected from the entire dataset. We grew 200 regression trees in our model runs, although error rates stabilized well before this number, and chose two random variables at each split for the results described below. The importance of each predictor variable was calculated by recording the mean-square error (sum of squared residuals divided by the number of observations) on the out-of-bag data for each tree and repeating that calculation after permuting each variable. The differences were averaged and normalized by the standard error giving an importance measure ranging from 0% to 100%. All analysis was done with the randomForest package (Liaw and Wiener 2002) in the R programming environment (R Development Core Team 2005).

4. Results

Approximately 2300×10^6 ha (68%) of the study area had sufficient satellite data to perform a trend analysis in the May–August window (all results are reported using the Vogelsang trend test; see the appendix). Fifteen percent of the individual time series grid cells, approximately 337×10^6 ha, showed significant trends in Pg, with 82% of the detected trends showing greening (Figure 1; Table 2). In many places the transition from areas of no significant slope to areas of positive slopes was associated with the ecotone into tundra vegetation or wetlands, while the areas of negative trends were almost exclusively in interior forests (Figure 2).

The majority of detrended 22-yr time series slopes registered neither greening nor browning for the May–August period. That observation held for the early period (May and June) and the late period (July and August) as well, but the proportion of positive to negative slopes changed, with browning occurring in approximately 136×10^6 ha during the July and August period as opposed to 36×10^6 ha in the earlier window (Table 2). Areas browning in the July and August window were largely confined to areas of interior forest in both continents, whereas tundra areas retained positive slopes (Figure 3). The spatial patterns of the significant slopes in May–June were similar to the entire growing season (May–August), but the slopes were steeper in the early period.

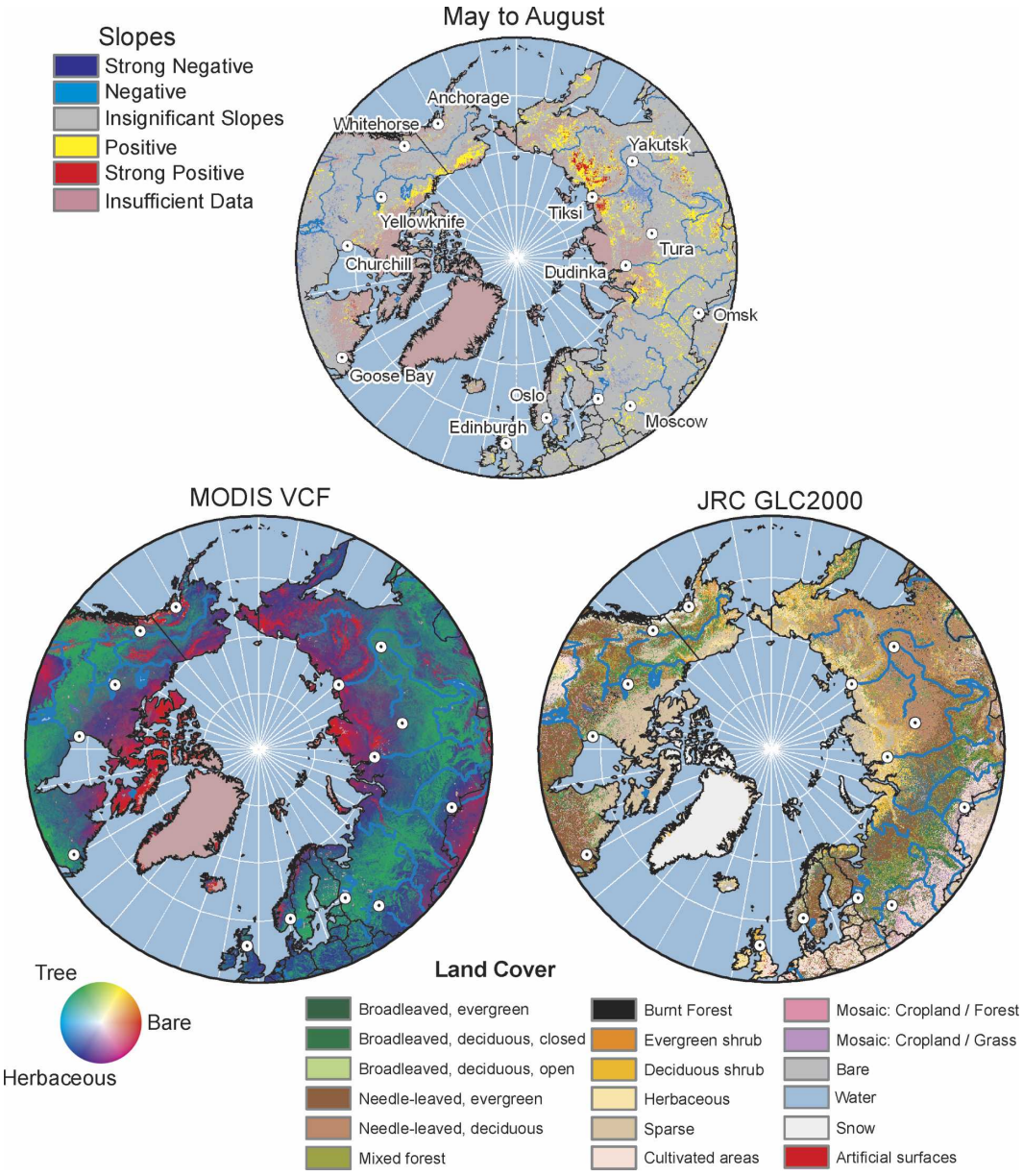

Figure 1. (top) Spatial distribution of significant deterministic trends in May–August photosynthetic activity from 1982 to 2003. The samples are colored according to the magnitude of the slope over time with greening areas shown in red and yellow and browning areas shown in shades of blue. Strongly negative regions are equivalent to a deterministic trend $\beta \leq -0.005$, negative regions $-0.005 < \beta \leq -0.0003$, near zero $-0.0003 < \beta \leq 0.0003$, and not significantly different than zero; positive $0.0003 < \beta \leq 0.005$; and strongly positive $\beta \geq 0.005$. (bottom) A false color composite of the MODIS VCF data and the GLC2000 land cover are shown for illustration of the distribution of trends.

Table 2. Areas of time series models of significant trends in Pg for three time windows. Percentages do not sum to 100% due to rounding.

	May–August × 10^6 ha		May–June × 10^6 ha		July–August × 10^6 ha	
No trend	2037	(86%)	2099	(88%)	2450	(86%)
Positive trends	277	(12%)	261	(11%)	255	(9%)
Negative trends	60	(3%)	36	(2%)	136	(5%)

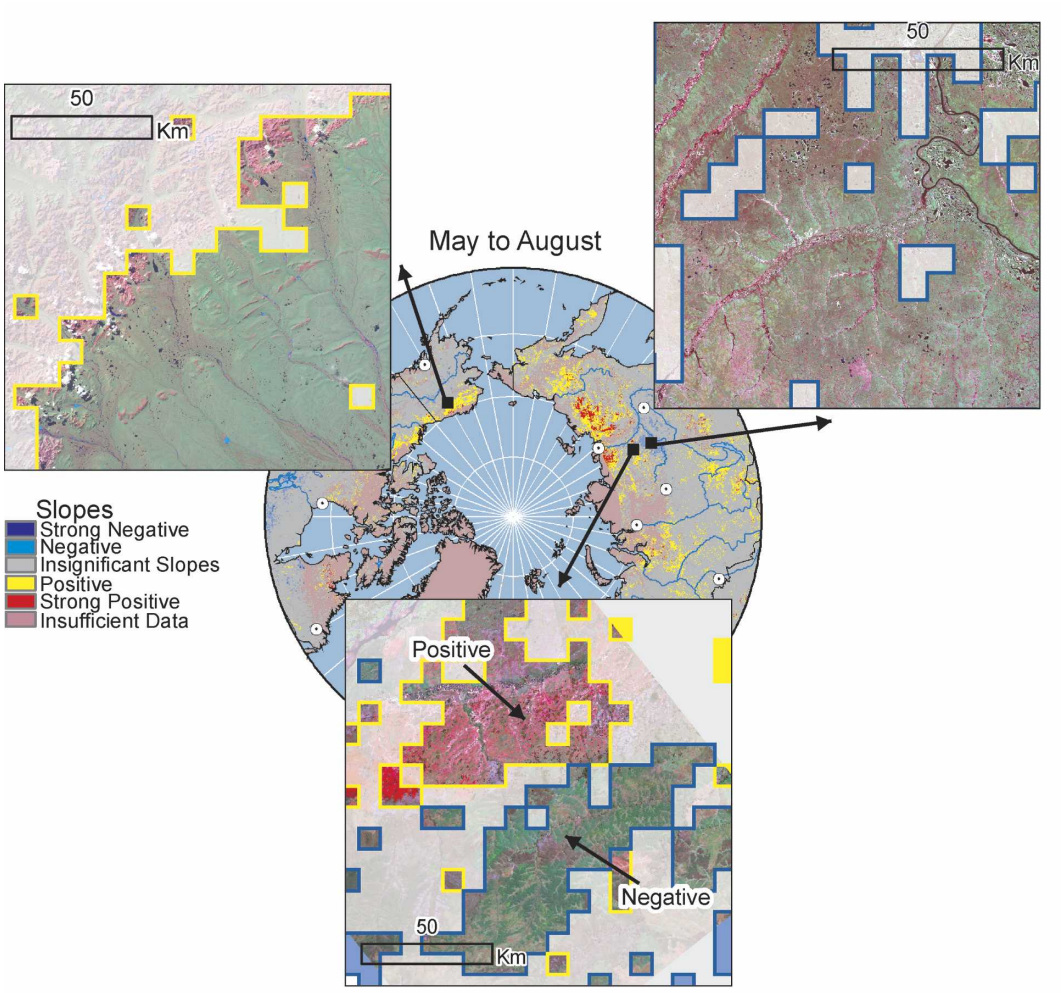

Figure 2. The trend map for May–August is shown with higher-resolution imagery from Landsat (30 m × 30 m cells) underlying three locations with characteristic trend patterns. Areas with significant trends are showing through while insignificant trends are opaque. The trends are colored according to magnitude as in Figure 1. (top left) The widespread greening occurring on the tundra areas north of the Brooks Range in Alaska (the mountains themselves show no significant trends). (top right) Negative trends in the interior forests of Russia. (bottom) A transition from positive to negative trends as a boundary from forest to wetlands is crossed.

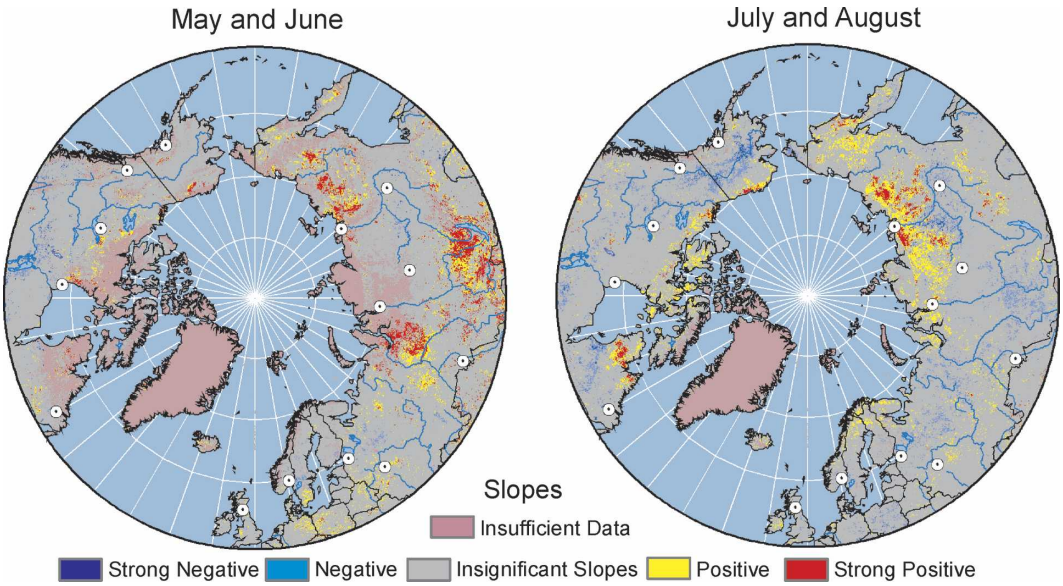

Figure 3. Spatial distribution of deterministic trends in photosynthetic activity from 1982 to 2003 for the early and late period of the growing season. Trends are colored according to magnitude as in Figure 1. Cities and rivers are as indicated in Figure 1.

These observations of different spatial patterns in the significant trends are supported by exploratory data analysis of the trend distribution by land cover and vegetation density as well as the ensemble regression tree models. The slope distributions (Figure 4) show that the major forest cover types tended to increase in greenness in the early part of the growing season and brown in the later half of the growing season, over the 22-yr record, while the tundra vegetation types greened during both halves of the growing season. For instance, the median values for significant slopes classified as "herbaceous" were positive in the early and late summer period while the median values for significant "needle-leaved evergreen" slopes shifted from positive to negative between the early and late summer periods. The exception to that pattern for the major forest types was needle-leaved deciduous forests, which had positive median slope values in both halves of the growing season. When the forest types were stratified by percent tree cover, then substantial areas of positive slopes in the second half of the growing season occurred only in the sparsest forests. The densest forests (>66% tree cover) had 3 to 10 times as many negative trends as positive trends in all three forest classes in July and August. Large areas of negative slopes, however, persisted in the sparsest (<33% tree cover) needle-leaved evergreen and broad-leaved deciduous forests (Figure 5). All the forest types showed a much greater proportion of greening slopes in the May–June window.

The randomForest models of trends (slopes) as a function of land cover and vegetation density were able to explain 48.3% of the variance using the out-of-bag error estimates in the May–August window. The models were able to explain only

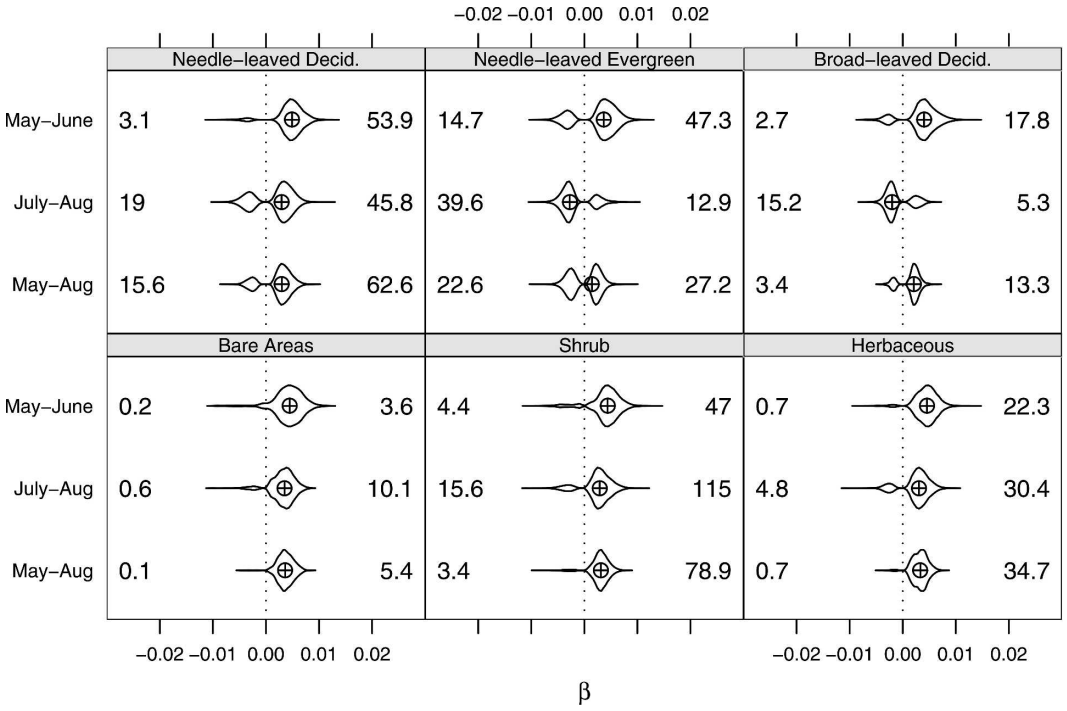

Figure 4. "Violin" plots show the distribution of significant slopes (*x* axis) for the time series models for (top row) major forest type and (bottom row) the major categories of low growing vegetation. Each panel is stratified by growing season window (*y* axis), and areas of either positive or negative slopes are shown as text in each panel in millions of hectares (10^6 ha). Violin plots are combinations of a box plot with rotated kernel density plot added to each side of the box plot (Hintze and Nelson 1998). Gaussian kernels were used with the bandwidth determined empirically using a bandwidth selector with a factor of 1.06 (Scott 1992).

28.3% of the variance in the first half of the growing season but 58.8% in the second half of the growing season. In all of the models land cover was the most important predictor variable in terms of the percent increase in mean-square errors (Figure 6). The percentage of tree cover was the second most important variable.

5. Discussion

The high latitudes have been warming substantially in recent decades (Easterling et al. 2000; Chapin et al. 2005; J. Hansen et al. 2005). It is generally thought that this warming will induce vegetation growth. In our analysis more than 85% of all areas show no significant trend in Pg over the 22-yr period since 1981 (Table 1), and the significant trends have distinct spatial patterns that correspond strongly to land cover (Figures 1 and 2). These observed trends in photosynthetic activity, as captured in the satellite data record, support previous analyses of greening in

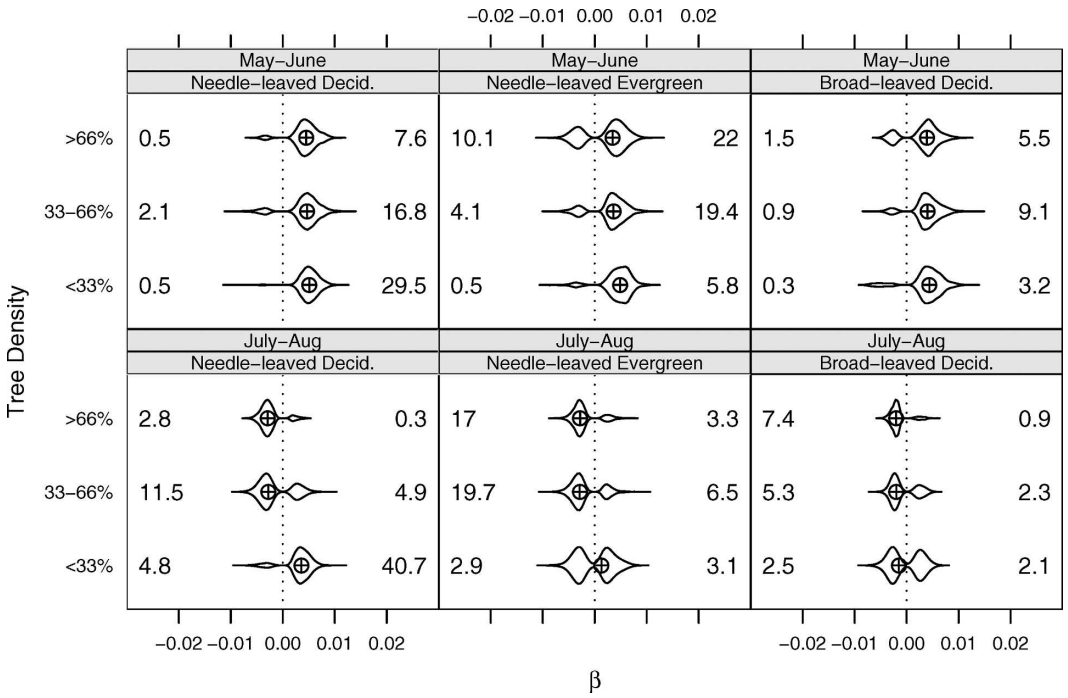

Figure 5. The distribution of significant slopes (*x* axis) for the time series models for (top row) the early part of the growing season and (bottom row) the later part of the growing season by forest type (columns). Each panel is further stratified by forest density (*y* axis), and areas of either positive or negative slopes are shown as text in each panel in millions of hectares (10^6 ha).

tundra vegetation, and enhance our understanding of the associations between trends in Pg, vegetation density, and cover type.

We used a robust series of trend tests to determine areas of significant greening, that is, positive trends in Pg from 1982 to 2003, and of significant browning—areas of decreasing photosynthetic activity. Because trend detection in biophysical systems requires consideration of autocorrelation and stationarity, we used three separate methods for assessing trends that have all been previously used on the AVHRR–NDVI data. The three trend tests produced the same general spatial patterns of greening and browning (see the appendix). The similar results across tests provide confidence in the robustness of the trend analysis. We emphasize the most conservative results, those from the Vogelsang test, although the conclusions of the study are consistent across all the trend tests.

Overall, tundra areas show marked greening over the entire May–August growing season, and indeed, the transition into tundra was typically delimited by a change in the time series from no significant trend to significant positive trends (Figure 2). This relationship held over all the time windows considered—tundra vegetation was almost exclusively greening in both the early and late growing season. These patterns were consistent with relatively simple climate response seen in a previous study across Canada (Bunn et al. 2005). In that study, tundra

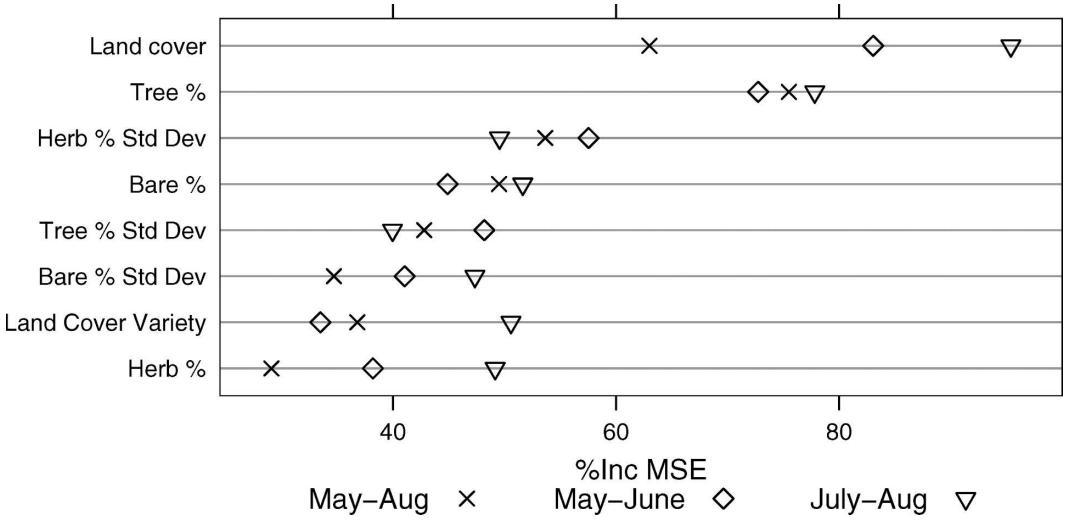

Figure 6. Variable importance plots for the randomForest models are shown for each time period (May–August, May and June, and July and August). The rows are sorted in order of mean increasing importance for all three time periods.

areas responded to summer maximum temperatures while the response of forest vegetation was more complex—generally relating to spring temperature and precipitation variables often from the previous year. The greening trends in tundra areas might also be associated with a lengthening of the growing season, and associated extension of the snow-free period, but characterizing phenology with the composited AVHRR–NDVI is limited by the compositing intervals (15 days) required to minimize the influence of clouds and other factors that modify the response to vegetation activity. The incidence of snow during the growing season would impact our results only if there were a systematic trend in snow cover over the time period we analyzed within the May–August growing season, which has not been the case (Brown 2000). Furthermore, analyses of the timing of snowmelt and vegetation activity represented by the NDVI confirm that these variables are nearly perfectly inversely related across a range of boreal forest sites (Delbart et al. 2005). Shrub expansion in response to climate across much of Alaska's tundra provides a separate line of evidence that supports the greening trends. Shrub density and area are rapidly expanding in Alaska in response to both summer temperatures and a positive feedback where increased shrub growth leads to increased snow-holding capacity, which, in turn, leads to increased microbial activity further facilitating growth (Sturm et al. 2001, 2005).

Boreal forest areas, in contrast, responded differently than tundra in both North America and northern Eurasia. Over the entire May–August growing season length, the trends in interior boreal forests were either balanced in terms of positive and negative Pg trends (e.g., needle-leaf evergreen forests showed approximately

27×10^6 ha greening and 23×10^6 ha browning; see Figure 4) or show a modest greening trend (e.g., needle-leaved deciduous and broad-leaved deciduous forests). Most forest areas showed significant greening trends in May and June, but our results indicated widespread evidence of reduced Pg (browning) in July and August. This pattern led a previous modeling study to conclude that large net photosynthetic gains are being made in the springtime in the northern extratropics that are then offset by net photosynthetic losses later in the summer (Angert et al. 2005).

These gross trends in greening or browning are, however, dependent not only on cover type (Figure 4) but also the underlying vegetation density (Figure 5). Areas of sparse tree cover (evergreen and deciduous) showed greening in July and August as well as May and June. In the needle-leaved deciduous class, some 40.6 $\times 10^6$ hectares of low-density "forest" were greening in a manner similar to the tundra vegetation that dominates this cover type. In contrast, more densely forested areas consistently displayed negative trends, particularly in late summer.

The boreal forest biome is ostensibly a temperature-limited ecosystem; the growing season is short and the winter is long and severe. The latitudinal tree line at global scales is related to minimum temperature, and tree line advance into tundra has been extensively documented (Lloyd 2005). Why then would rising temperatures result in declining gross photosynthesis in boreal forests? Pronounced warming has already occurred at high northern latitudes over the last half-century (Easterling et al. 2000), and Arctic summers are now warmer than at any other time in the last 400 yr (Overpeck et al. 1997). From 1954 to 2003, high northern latitudes warmed by as much as 2°–3°C (ACIA 2004), and the rate of warming has increased in recent decades: high latitudes warmed at the rate of 0.15°–0.17°C decade^{-1} between 1961 and 1993 (Chapman and Walsh 1993), and might be increasing as much as to 0.3°–0.4°C decade^{-1} through 2004 (Chapin et al. 2005). Despite some evidence for an overall increase in precipitation (Serreze et al. 2000), there is also evidence for evaporative drying in the Arctic, suggesting that seasonal drought conditions to which the vegetation are not well adapted might prevail in these high-latitude ecosystems (Yoshikawa and Hinzman 2003; Dai et al. 2004). Summer drought stress can be induced by both lower local precipitation as well as increased evapotranspiration demands driven by the increases in temperature. The key to the lack of widespread increases in boreal forest growth and its decline over large areas is, we hypothesize, likely due to temperature-induced drought stress expressed as vapor pressure deficit limiting boreal conifer photosynthesis. This observation is supported by CO_2 flux measurements of boreal conifers (Jarvis et al. 1997), longer-term changes in allocation across boreal tree species (Lapenis et al. 2005), and studies conducted using tree-ring proxies of tree growth. The latter document negative correlations between summer temperatures and ring widths associated with summer drought (Barber et al. 2000; Lloyd and Fastie 2002; Wilmking et al. 2004).

An alternate explanation that might lead to negative trends in boreal forest Pg is fire, as burned area frequency has been increasing over the last 20 yr (Achard et al. 2005; Mouillot and Field 2005). Analysis of fire disturbance was not conducted in the current analysis owing to the lack of reliable burned area assessments over the entire record (Sukhinin et al. 2004) but a related study of boreal North America (Goetz et al. 2005), for which detailed burned area maps were available,

showed that fire was not associated with negative Pg trends. Instead, temporal trends in the burned area were predominantly stochastic, as would be expected except for areas disturbed at the beginning of the time series.

These results, and earlier work that led to this analysis (Goetz et al. 2005), were initially surprising to us given the abundant indications of Northern Hemisphere greening and increased productivity in recent decades (Myneni et al. 1997; Zhou et al. 2001; Nemani et al. 2003; Slayback et al. 2003). Our results indicate that the majority of the northern high latitudes have not consistently increased in Pg over the record and indeed Pg has declined in many forested areas. There is emerging evidence that the productivity of high-latitude forests might decline with climate warming due to drought (Angert et al. 2005), transitions in species composition (ACIA 2004), and other factors (see Goetz et al. 2005). It is not yet certain that these trends will continue as climate continues to warm in these high latitudes, or if other surprises might modify the feedback mechanisms between vegetation and the atmosphere. Recent analyses of boreal tree-ring records indicate the potential of merging the extensive dendrochronology network with the satellite observational record (Kaufmann et al. 2004), which would help to place these results into a longer-term context. It would also provide insight into potential limitations of ecosystem process models that, until recently, have missed these apparent biospheric responses to climatic change.

Acknowledgments. We gratefully acknowledge support from the NOAA Carbon Cycle Science Program, and earlier support from the NASA ADRO program that led to this analysis. We thank Simon Hay for guidance on the time series analysis, Jen Small for programming the original time series source code (Small et al. 2003), and Jim Tucker's GIMMS group for providing their AVHRR dataset.

Appendix

Alternate Trend Tests

We performed three separate trend tests, as described in section 3 above: a nonparametric trend test (Siegel and Castellan 1988), the Augmented Dickey Fuller (ADF) test (Dickey and Fuller 1981), and Vogelsang's $t\text{-}PS_T$ stationarity test (Vogelsang 1998; Fomby and Vogelsang 2002). Each test has been used in various applications, and different analysts describe their relative strengths and weaknesses elsewhere. All are somewhat limited by the relatively short segment length of the AVHRR–NDVI time series (22 yr), but each captured the same general spatial pattern for significant trends (Figure A1). We elected to focus on the results of the Vogelsang test for the analysis reported in the main text because it has been shown to be robust to spurious trends that result from serial correlation and does not overreject the hypothesis of no trend (Vogelsang 1998; Fomby and Vogelsang 2002). The areas identified as showing deterministic greening and browning trends vary somewhat depending on the test used, primarily with the level of significance rather than with the location or direction of the identified trends (Figure A1). The overall results of the analysis, in terms of the relative proportion of significant positive or negative trends in different land cover types and vegetation densities, do not change with the test used.

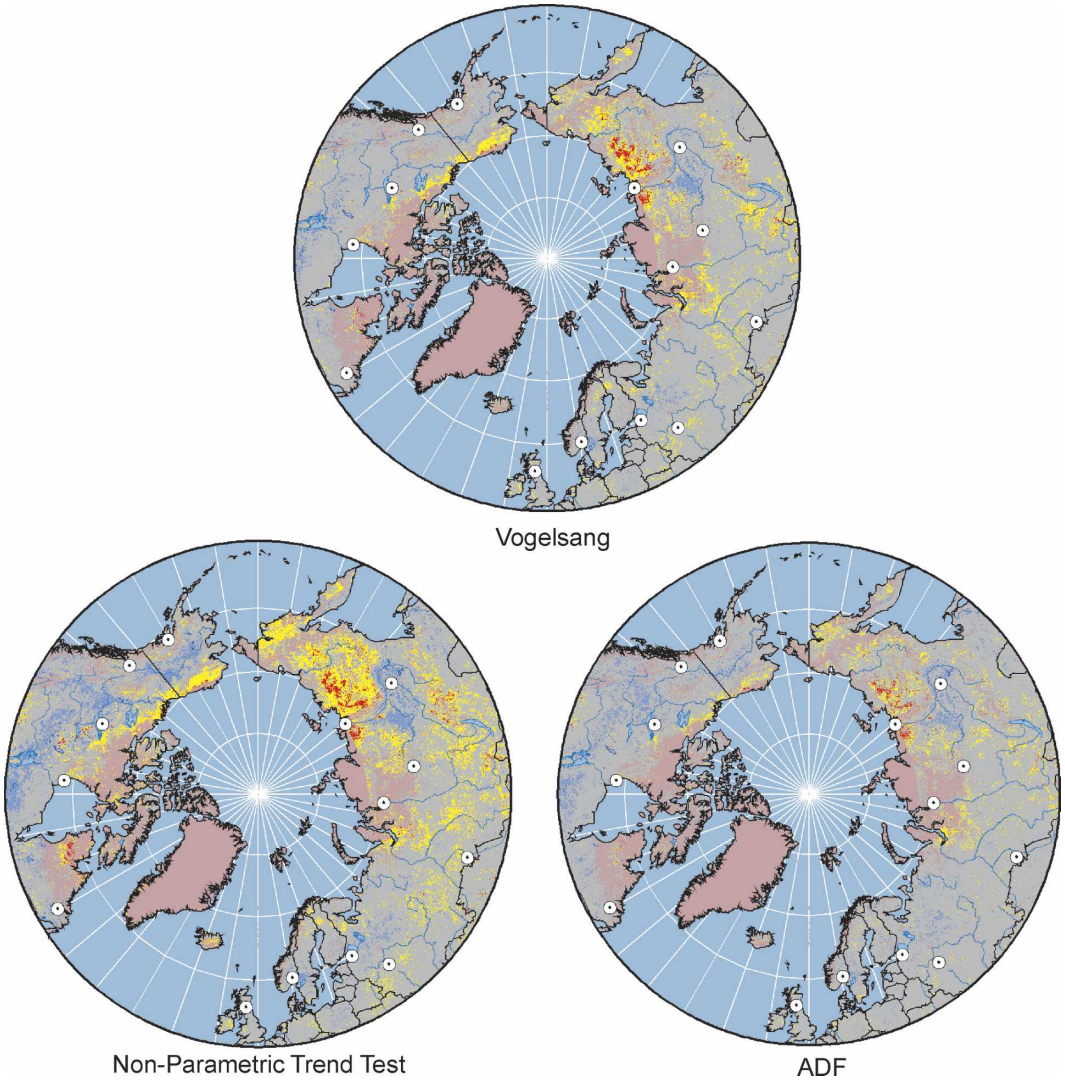

Figure A1. The spatial distribution of significant deterministic trends in May–August photosynthetic activity from 1982 to 2003 for the three trend detection tests used. (top) The Vogelsang test, which was used for the analyses described in the main body of the paper. (bottom) The nonparametric trend test and the ADF are shown for comparison. The samples are colored according to the magnitude of the slope over time with greening areas shown in red and yellow and browning areas shown in shades of blue. Strongly negative regions are equivalent to a deterministic trend $\beta \leq -0.005$, negative regions $-0.005 < \beta \leq -0.0003$, near zero $-0.0003 < \beta \leq 0.0003$, and not significantly different than zero; positive $0.0003 < \beta \leq 0.005$; and strongly positive $\beta \geq 0.005$.

References

Achard, F., H.-J. Stibig, L. Laestadius, V. Roshchanka, A. Yaroshenko, and D. Aksenov, 2005: Identification of "hot spot areas" of forest cover changes in boreal Eurasia. [Available online at http://www-tem.jrc.it//PDF_publis/2005/Achard&al_HotSpot-Boreal-Eurasia.pdf.]

ACIA, 2004: *Impacts of a Warming Arctic—Arctic Climate Impact Assessment Overview Report: Overview Report*. Cambridge University Press, 144 pp.

Aksenov, D., and Coauthors, 2002: *Atlas of Russia's Intact Forest Landscapes*. World Resources Institute, 72 pp.

Angert, A., S. Biraud, C. Bonfils, C. C. Henning, W. Buermann, J. Pinzon, C. J. Tucker, and I. Fung, 2005: Drier summers cancel out the CO_2 uptake enhancement induced by warmer springs. *Proc. Natl. Acad. Sci. USA,* **102,** 10 823–10 827.

Asrar, G., M. Fuschs, E. T. Kanemasu, and J. L. Hatfield, 1984: Estimating absorbed photosynthetic radiation and leaf area index from spectral reflectance in wheat. *Agron. J.,* **76,** 300–306.

——, E. T. Kanemasu, R. D. Jackson, and P. J. Pinter, 1985: Estimation of total above ground phytomass production using remotely sensed data. *Remote Sens. Environ.,* **17,** 211–220.

Barber, V. A., G. P. Juday, and B. P. Finney, 2000: Reduced growth of Alaskan white spruce in the twentieth century from temperature-induced drought stress. *Nature,* **405,** 668–673.

Bartalev, S. A., A. S. Belward, D. V. Erchov, and A. S. Isaev, 2003: A new Spot4-Vegetation Derived Land Cover Map of northern Eurasia. *Int. J. Remote Sens.,* **24,** 1977–1982.

Bonan, G. B., D. Pollard, and S. L. Thompson, 1992: Effects of boreal forest vegetation on global climate. *Nature,* **359,** 716–718.

Breiman, L., 1996: Bagging predictors. *Mach. Learn.,* **24,** 123–140.

——, 2001: Random forests. *Mach. Learn.,* **45,** 5–32.

Brown, M. E., J. E. Pinzon, and C. J. Tucker, 2004: New vegetation index data set to monitor global change. *Eos, Trans. Amer. Geophys. Union,* **85,** 565–569.

Brown, R. D., 2000: Northern Hemisphere snow cover variability and change, 1915–1997. *J. Climate,* **13,** 2339–2355.

Bunn, A. G., S. J. Goetz, and G. J. Fiske, 2005: Observed and predicted responses of plant growth to climate across Canada. *Geophys. Res. Lett.,* **32,** L16710, doi:10.1029/2005GL023646.

Chapin, F. S., and Coauthors, 2005: Role of land-surface changes in Arctic summer warming. *Science,* **310,** 657–660.

Chapman, W. L., and J. E. Walsh, 1993: Recent variations of sea ice and air temperature in high latitudes. *Bull. Amer. Meteor. Soc.,* **74,** 33–47.

Cox, P. M., R. A. Betts, C. D. Jones, S. A. Spall, and I. J. Totterdell, 2000: Acceleration of global warming due to carbon-cycle feedbacks in a coupled climate model. *Nature,* **408,** 184–187.

Dai, A., K. E. Trenberth, and T. Qian, 2004: A global dataset of Palmer Drought Severity Index for 1870–2002: Relationship with soil moisture and effects of surface warming. *J. Hydrometeor.,* **5,** 1117–1130.

Daughtry, C. S. T., K. P. Gallo, S. N. Goward, S. D. Prince, and W. P. Kustas, 1992: Spectral estimates of absorbed radiation and phytomass production in corn and soybean canopies. *Remote Sens. Environ.,* **39,** 141–152.

Defries, R. S., M. C. Hansen, and J. R. G. Townshend, 2000: Global continuous fields of vegetation characteristics: A linear mixture model applied to multi-year 8 km AVHRR data. *Int. J. Remote Sens.,* **21,** 1389–1414.

Delbart, N., L. Kergoat, T. Le Toan, J. Lhermitte, and G. Picard, 2005: Determination of phenological dates in boreal regions using Normalized Difference Water Index. *Remote Sens. Environ.,* **97,** 26–38.

Dickey, D. A., and W. A. Fuller, 1981: Likelihood ratio statistics for autoregressive time series with a unit root. *Econometrica,* **49,** 1057–1072.

Dufresne, J. L., P. Friedlingstein, M. Berthelot, L. Bopp, P. Ciais, L. Fairhead, H. Le Treut, and P.

Monfray, 2002: On the magnitude of positive feedback between future climate change and the carbon cycle. *Geophys. Res. Lett.,* **29,** 1405, doi:10.1029/2001GL013777.

Easterling, D. R., T. R. Karl, K. P. Gallo, D. A. Robinson, K. E. Trenberth, and A. Dai, 2000: Observed climate variability and change of relevance to the biosphere. *J. Geophys. Res.,* **105D,** 20 101–20 114.

Field, C., 1991: Ecological scaling of carbon gain to stress and resource availability. *Response of Plants to Multiple Stresses*, H. A. Mooney, W. E. Winner, and E. J. Pell, Eds., Academic Press, 35–65.

Fomby, T. B., and T. J. Vogelsang, 2002: The application of size-robust trend statistics to global-warming temperature series. *J. Climate,* **15,** 117–123.

Giri, C., Z. Zhu, and B. Reed, 2005: A comparative analysis of the Global Land Cover 2000 and MODIS land cover data sets. *Remote Sens. Environ.,* **94,** 123–132.

Goel, N., and W. Qin, 1994: Influence of canopy architecture on various vegetation indices and Lai and Fpar: Simulation model results. *Remote Sens. Rev.,* **10,** 309–347.

Goetz, S. J., and S. D. Prince, 1998: Variability in carbon exchange and light utilization among boreal forest stands: Implications for remote sensing of net primary production. *Can. J. For. Res.,* **28,** 375–389.

——, and ——, 1999: Modeling terrestrial carbon exchange and storage: Evidence and implications of functional convergence in light use efficiency. *Adv. Ecol. Res.,* **28,** 57–92.

——, A. G. Bunn, G. J. Fiske, and R. A. Houghton, 2005: Satellite-observed photosynthetic trends across boreal North America associated with climate and fire disturbance. *Proc. Natl. Acad. Sci. USA,* **102,** 13 521–13 525.

Gorham, E., 1991: Northern peatlands—Role in the carbon-cycle and probable responses to climatic warming. *Ecol. Appl.,* **1,** 182–195.

Hansen, J., and Coauthors, 2005: Earth's energy imbalance: Confirmation and implications. *Science,* **308,** 1431–1435.

Hansen, M. C., R. S. DeFries, J. R. G. Townshend, L. Marufu, and R. Sohlberg, 2002a: Development of a MODIS tree cover validation data set for Western Province, Zambia. *Remote Sens. Environ.,* **83,** 320–335.

——, ——, ——, R. Sohlberg, C. Dimiceli, and M. Carroll, 2002b: Towards an operational MODIS continuous field of percent tree cover algorithm: Examples using AVHRR and MODIS data. *Remote Sens. Environ.,* **83,** 303–319.

——, J. R. G. Townshend, R. S. Defries, and M. Carroll, 2005: Estimation of tree cover using MODIS data at global, continental and regional/local scales. *Int. J. Remote Sens.,* **26,** 4359–4380.

Hintze, J. L., and R. D. Nelson, 1998: Violin plots: A box plot-density trace synergism. *Amer. Stat.,* **52,** 181–184.

Jarvis, P. G., J. M. Massheder, S. E. Hale, J. B. Moncrieff, M. Rayment, and S. L. Scott, 1997: Seasonal variation of carbon dioxide, water vapor, and energy exchanges of a boreal black spruce forest. *J. Geophys. Res.,* **102D,** 28 953–28 966.

Kaufmann, R. K., R. D. D'Arrigo, C. Laskowski, R. B. Myneni, L. Zhou, and N. K. Davi, 2004: The effect of growing season and summer greenness on northern forests. *Geophys. Res. Lett.,* **31,** L09205, doi:10.1029/2004GL019608.

Keeling, C. D., J. F. S. Chin, and T. P. Whorf, 1996: Increased activity of northern vegetation inferred from atmospheric CO_2 measurements. *Nature,* **382,** 146–149.

Lapenis, A., A. Shvidenko, D. Shepaschenko, S. Nilsson, and A. Aiyyer, 2005: Acclimation of Russian forests to recent changes in climate. *Global Change Biol.,* **11,** 2090–2102.

Latifovic, R., Z. L. Zhu, J. Cihlar, C. Giri, and I. Olthof, 2004: Land cover mapping of North and Central America—Global Land Cover 2000. *Remote Sens. Environ.,* **89,** 116–127.

Lawrence, R., A. Bunn, S. Powell, and M. Zambon, 2004: Classification of remotely sensed imagery using stochastic gradient boosting as a refinement of classification tree analysis. *Remote Sens. Environ.,* **90,** 331–336.

——, S. D. Wood, and R. L. Sheley, 2006: Mapping invasive plants using hyperspectral imagery and the random forest algorithm. *Remote Sens. Environ.,* **100,** 356–362.

Liaw, A., and M. Wiener, 2002: Classification and regression by randomForest. *R News,* Vol. 2, No. 3, 18–22.

Lloyd, A. H., 2005: Ecological histories from Alaskan tree lines provide insight into future change. *Ecology,* **86,** 1687–1695.

——, and C. L. Fastie, 2002: Spatial and temporal variability in the growth and climate response of treeline trees in Alaska. *Climate Change,* **52,** 481–509.

Mouillot, F., and C. B. Field, 2005: Fire history and the global carbon budget: A 1° × 1° fire history reconstruction for the 20th century. *Global Change Biol.,* **11,** 398–420.

Myneni, R. B., F. G. Hall, P. J. Sellers, and A. L. Marshak, 1995: The interpretation of spectral vegetation indexes. *IEEE Trans. Geosci. Remote Sens.,* **33,** 481–486.

——, C. D. Keeling, C. J. Tucker, G. Asrar, and R. R. Nemani, 1997: Increased plant growth in the northern high latitudes from 1981 to 1991. *Nature,* **386,** 698–702.

Nemani, R. R., C. D. Keeling, H. Hashimoto, W. M. Jolly, S. C. Piper, C. J. Tucker, R. B. Myneni, and S. W. Running, 2003: Climate-driven increases in global terrestrial net primary production from 1982 to 1999. *Science,* **300,** 1560–1563.

Nikolauk, V. A., 1973: *Atlas of Forestry of USSR*. State Committee of Forestry and Forestry Management of Soviet Ministry of USSR, 222 pp.

Overpeck, J., and Coauthors, 1997: Arctic environmental change of the last four centuries. *Science,* **278,** 1251–1256.

R Development Core Team, cited 2005: R: A language and environment for statistical computing. [Available online at http://www.R-project.org.]

Richardson, A. J., and C. L. Wiegand, 1977: Distinguishing vegetation from soil background information. *Photogramm. Eng. Remote Sens.,* **43,** 1541–1552.

Ryan, M. G., M. B. Lavigne, and S. T. Gower, 1997: Annual carbon cost of autotrophic respiration in boreal forest ecosystems in relation to species and climate. *J. Geophys. Res.,* **102D,** 28 871–28 883.

Scott, D. W., 1992: *Multivariate Density Estimation: Theory, Practice, and Visualization*. Wiley, 336 pp.

Sellers, P. J., 1987: Canopy reflectance, photosynthesis and transpiration. II. The role of biophysics in the linearity of their interdependence. *Remote Sens. Environ.,* **21,** 143–183.

Serreze, M. C., and Coauthors, 2000: Observational evidence of recent change in the northern high-latitude environment. *Climate Change,* **46,** 159–207.

Siegel, S., and N. J. Castellan, 1988: *Non-Parametric Statistics*. McGraw-Hill, 399 pp.

Slayback, D. A., J. E. Pinzon, S. O. Los, and C. J. Tucker, 2003: Northern Hemisphere photosynthetic trends 1982–99. *Global Change Biol.,* **9,** 1–15.

Small, J., S. J. Goetz, and S. I. Hay, 2003: Climatic suitability for malaria transmission in Africa, 1911–1995. *Proc. Natl. Acad. Sci. USA,* **100,** 15 341–15 345.

Spanner, M. A., L. L. Pierce, S. W. Running, and D. L. Peterson, 1990: The seasonality of AVHRR data of temperate coniferous forests—Relationship with Leaf-Area Index. *Remote Sens. Environ.,* **33,** 97–112.

Steinberg, D. C., S. J. Goetz, and E. Hyer, 2006: Validation of MODIS Fpar products in boreal forests of Alaska. *IEEE Trans. Geosci. Remote Sens.,* in press.

Sturm, M., J. P. McFadden, G. E. Liston, F. S. Chapin, C. H. Racine, and J. Holmgren, 2001: Snow–shrub interactions in arctic tundra: A hypothesis with climatic implications. *J. Climate,* **14,** 336–344.

——, J. Schimel, G. Michaelson, J. M. Welker, S. F. Oberbauer, G. E. Liston, J. Fahnestock, and V. E. Romanovsky, 2005: Winter biological processes could help convert arctic tundra to shrubland. *Bioscience,* **55,** 17–26.

Sukhinin, A. I., and Coauthors, 2004: AVHRR-based mapping of fires in Russia: New products for fire management and carbon cycle studies. *Remote Sens. Environ.,* **93,** 546–564.

Tucker, C. J., 1979: Red and photographic infrared linear combinations for monitoring vegetation. *Remote Sens. Environ.,* **8,** 127–150.

——, B. N. Holben, J. H. Elgin, and J. E. McMurtry, 1981: Remote sensing of total dry matter accumulation in winter wheat. *Remote Sens. Environ.,* **11,** 171–189.

——, J. E. Pinzon, M. E. Brown, D. Slayback, E. W. Pak, R. Mahoney, 2005: An extended AVHRR 8-km NDVI data set compatible with MODIS and spot vegetation NDVI data. *Int. J. Remote Sens.,* **26,** 4485–4498.

Turner, D. P., S. Urbanski, D. Bremer, S. C. Wofsy, T. Meyers, S. T. Gower, and M. Gregory, 2003: A cross-biome comparison of daily light use efficiency for gross primary production. *Global Change Biol.,* **9,** 383–395.

Vogelsang, T. J., 1998: Trend function hypothesis testing in the presence of serial correlation. *Econometrica,* **66,** 123–148.

Wilmking, M., G. P. Juday, V. A. Barber, and H. S. J. Zald, 2004: Recent climate warming forces contrasting growth responses of white spruce at treeline in Alaska through temperature thresholds. *Global Change Biol.,* **10,** 1724–1736.

Yoshikawa, K., and L. D. Hinzman, 2003: Shrinking thermokarst ponds and groundwater dynamics in discontinuous permafrost near Council, Alaska. *Permafrost Periglac. Processes,* **14,** 151–160.

Zhou, L. M., C. J. Tucker, R. K. Kaufmann, D. Slayback, N. V. Shabanov, and R. B. Myneni, 2001: Variations in northern vegetation activity inferred from satellite data of vegetation index during 1981 to 1999. *J. Geophys. Res.,* **106D,** 20 069–20 083.